The Japan Society
of Applied Physics

LETTER • OPEN ACCESS

Externally triggerable optical pump-probe scanning tunneling microscopy

View the article online for updates and enhancements.

Externally triggerable optical pump-probe scanning tunneling microscopy

Hiroyuki Mogi[†], Zi-han Wang[†], Ryusei Kikuchi, Cheul Hyun Yoon, Shoji Yoshida, Osamu Takeuchi, and Hidemi Shigekawa[*]

Faculty of Pure and Applied Sciences, University of Tsukuba, Tsukuba, 305-8573, Japan

[*]E-mail: hidemi@ims.tsukuba.ac.jp
[†]These two authors contributed equally to this work.

Optical pump-probe scanning tunneling microscopy (OPP-STM) has enabled the measurement of ultrafast dynamics in real space. However, the use of a pulse picker to extract selected laser pulses to realize delay-time modulation, which efficiently suppresses the thermal expansion problems, limits the availability of time-resolved measurement. Here, we present a more applicable type of OPP-STM that we have developed. Two externally triggerable pulse lasers were used to produce pump and probe pulses, and wide-range delay-time modulation was simply realized by adjusting the timing of the pulses. The performance of this new type of OPP-STM was demonstrated by measuring the carrier dynamics in WSe_2. © 2019 The Japan Society of Applied Physics

It is very important to measure and evaluate the dynamics in nanoscale materials and devices for further advances in the development of desired functions. Optical pump-probe (OPP) methods[1] have excellent time resolution for such purposes. However, for an in-depth understanding of the dynamics, simultaneous analysis in the spatial domain with the time-resolved measurement is a key factor. For this purpose, time-resolved techniques for simultaneous use with methods such as electron microscopy,[2] photoemission electron microscopy,[3] and diffraction methods[4] have been devised. Scanning tunneling microscopy/spectroscopy (STM/STS) is a promising technique for visualizing, characterizing, and manipulating solid surfaces/interfaces at the atomic scale.[5] However, its temporal resolution is in the sub-millisecond range owing to the limitation imposed by the preamplifier bandwidth, and considerable effort has been made to improve the temporal resolution since its invention.[6–9]

Recently, by combining STM with optical pump-probe (OPP) methods, STM methods with a higher time resolution have been developed.[10–12] In OPP methods, to accurately measure small changes in a signal, usually the pump light intensity is modulated and the change in the signal corresponding to the modulation is detected by the lock-in method. When OPP methods are combined with STM, however, thermal expansion of the tip and sample occurs when the light intensity changes. Since a 0.1 nm change in the tunnel gap (tip-sample distance) causes a one-order change in tunnel current, this has impeded the combination of STM with OPP methods (OPP-STM). Therefore, a modulation technique different to those used in the conventional OPP methods has been desired. One of the promising techniques is the delay-time modulation.[13]

In OPP-STM with delay-time modulation, the pulse width of the laser determines the time resolution, and the modulation amplitude of the delay time determines the measurable physical phenomena. If only small amplitudes can be realized, only ultrafast physical phenomena can be measured, but if both small and large amplitudes can be realized, it becomes possible to measure a wide range of physical phenomena with ultrafast to relatively slow dynamics. Also, the frequency of the delay-time modulation affects the measurement accuracy. Generally, a signal from a measuring device contains a noise component whose amplitude is inversely proportional to the frequency f ($1/f$ noise).

When the modulation frequency is too low, a large noise remains in the signal after lock-in detection. Therefore, it is desirable that the modulation frequency is set to 1 kHz or higher.

We previously introduced the following two types of pump-probe generator capable of delay-time modulation. (1) A type that mechanically moves a mirror to change the optical path length.[14] (2) A type that uses specific pulse pairs extracted from a pulse train by a pulse picker such as a Pockels cell.[15,16] The first type can be realized relatively easily when the modulation amplitude is small. However, to realize an amplitude exceeding 100 ps, an optical path length on the order of 10 cm must be instantaneously changed, and it becomes impossible to achieve a fast delay-time modulation mechanically. On the other hand, the second type can easily realize delay-time modulation by a large amplitude of about 1 μs with a modulation frequency of 10 kHz or more. However, to achieve a high time resolution, it is necessary to synchronize the oscillations of the two lasers, and a pulse picker, a circuit for driving it, a cooling system and other various optical elements are required, making the system rather complicated and not so easy to use. In the case of OPP-STM, a stability much higher than the case of the conventional OPP method is required. In addition, since an ultrafast pulse picker used in our system, integrated with an RTP crystal (LEYSOP, RTP-3-20) operating at 1 MHz, generally has a limited extinction ratio of 250:1,[17] some of the light other than the selected (picked) and transmitted light also passes through, which has an adverse effect on the measurement of some object.[18]

With the above perspective, here we present a newly developed OPP-STM system that utilizes externally triggerable pulse lasers, which we call externally triggerable OPP-STM (ET-OPP-STM). Figure 1 shows a schematic illustration of the designed system. The system simply consists of two lasers, which can generate optical pulses immediately after an electric pulse is input at an arbitrary timing, and a specifically designed signal generator. This simple setup with fewer optical elements makes the system stable, compact, and easy to use.

It is desirable that the repetition period from one pulse to the next be short and that the fluctuation of the delay time from the input of the electric signal to the output of the light pulse (timing jitter) is small. An FPGA, for example, can be used to control the signal generation. It is possible to operate

(a)

(b)
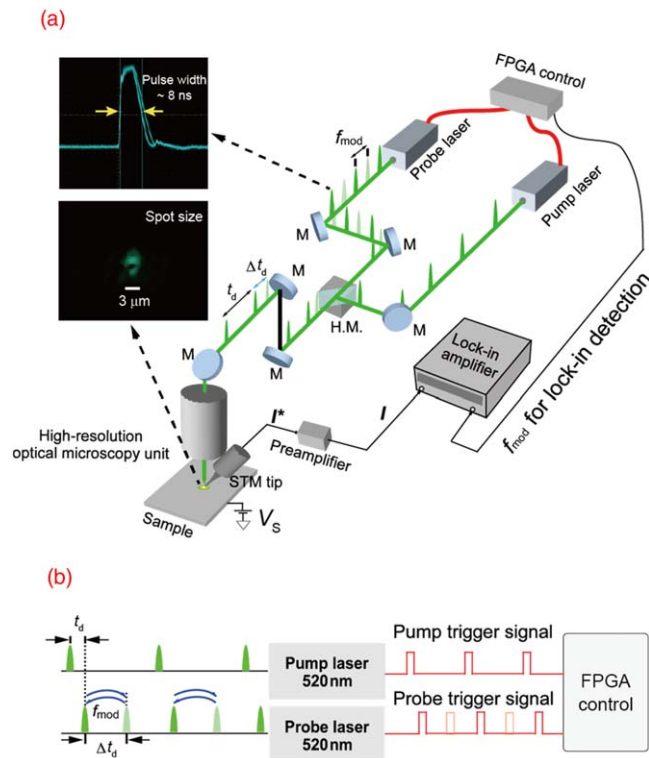
Fig. 1. (Color online) (a) Schematic illustration of the developed OPP-STM system. The system consists of two lasers with a nanosecond pulse width of ~8 ns, which can generate an optical pulse immediately after the input of an electric pulse at an arbitrary timing, and a signal generator. A field-programmable gate array (FPGA) was used to control the signal generation. A high-resolution optical microscope (~1 μm spatial resolution) with an optical access port was attached outside the main UHV chamber of the STM system, which was oriented perpendicular to the sample plate. This particular design not only provides a way of checking the locations of the sample surface and tip, but has excellent laser focusability. The STM tip was attached diagonally, so that its apex can be more clearly seen from above. The light spot size observed by the optical microscope and the form of the laser pulse produced are shown together. (b) Schematic of delay-time modulation. The delay time between the pump and probe pulses was modulated between t_d and $t_d + \Delta t_d$ at ~1 kHz. Here, a simple type of modulation realized by adjusting the timing of the probe pulse generation is shown. M, mirror; H.M., half mirror; t_d, delay time between the pump and probe pulses; Δt_d; difference between two delay times used for modulation; V_s, sample bias voltage; f_{mod}, delay-time modulation frequency; I, raw tunnel current; I^*, signal current averaged by preamplifier.

the internal circuit with a clock frequency of about 200 MHz–2 GHz using a recently produced commercial FPGA, and it is possible to control the timing of the generation of the electric pulse with a time resolution of 0.5–5 ns by only using the embedded clock synchronization circuit. Furthermore, depending on the FPGA, the output section includes an output delay circuit with a resolution of the order of 10 ps, and by combining this section with a clock synchronization circuit, the timing of the generation of the electric pulse can be controlled with a resolution of the order of 10 ps. If necessary, it is also possible to add an analog delay circuit that can be adjusted with a ps-order resolution. Thus, by changing this delay time from the FPGA, it is possible to generate electric pulses with ps-order resolution.

Although it is possible to have a ns or ps optical pulse width, the case of a ns pulse width is described here to simply enable a comparison with the previous result obtained using the original OPP-STM system.[19] Here, two thermally

stabilized diode systems (Thorlabs, NPL52B) with a central wavelength at 520 nm and nanosecond pulse width (~8 ns) were used. By taking advantage of the external triggerability, one can determine the repetition rate f_{rep} of each laser solely by the frequency of the input electrical trigger pulse. f_{rep} for the laser was electrically adjusted from 1 kHz to 10 MHz in the current case. On this basis, the two lasers were easily synchronized in terms of f_{rep} by feeding them with two trigger pulses (pump trigger and probe trigger) with an identical frequency. This synchronization scheme provides a simple and efficient way of freely tuning the optical delay time t_d between the pump and probe pulses. The probe trigger is intentionally (electronically) delayed with respect to the pump trigger by up to $t_d = 1/(2 \times f_{rep})$. The sweeping of t_d back and forth at a designated speed is also achievable. In addition, the delay-time modulation is also easily realized: the delay time can be modulated between t_d and $t_d + \Delta t_d$ ($<1/(2 \times f_{rep})$) at a desired frequency f_{mod} (~1 kHz) without the pulse-picking technique.

Next, time-resolved experiments were carried out by measuring the carrier dynamics in a WSe$_2$ sample. Note that an STM system with special design was adopted: a high-resolution optical microscope (~1 μm spatial resolution) with an optical access port was attached outside the main UHV chamber of the STM system, which was oriented perpendicular to the sample plate. This particular design not only provides a way of checking the locations of the sample surface and tip, but has excellent laser focusability (~3 μm in this case). The STM tip was attached diagonally, as shown in Fig. 1, so that its apex can be more clearly seen from above.

WSe$_2$, a typical indirect-bandgap semiconductor with a relatively long carrier recombination lifetime (~2 μs),[20] was chosen as a sample. Since OPP-STM measurement has already been carried out on this material, it is suitable for demonstrating the performance of ET-OPP-STM, by comparison with the results obtained by OPP-STM. In the previous OPP-STM measurement, two components with lifetimes of ns and 100 ns order were observed. Since the recombination lifetime was ~2 μs, these components were respectively attributed to rapid tunneling of excess minority carriers transiently trapped at the surface and the photocurrent dynamics reflecting the flow of excited photocarriers at the surface, whose lifetime is determined by the balance between the diffusion/drift and tunneling rates. In OPP-STM with the pulsed light selected by pulse picking (1 MHz) from a pulse train of 90 MHz, the maximum delay time was $1/(2 \times 1\text{ MHz}) = \sim500$ ns. Although the excess electrons trapped at the surface, which are difficult to measure by other methods, were successfully detected, it was not possible to obtain information on the slow recombination lifetime of electrons (~2 μs). In fact, when the light intensity was high, relaxation had not been completed even at 400 ns, namely because although the existence of a long-lifetime component was indicated, it could not be observed. Therefore, this sample was used as a measurement target to demonstrate the performance of ET-OPP-STM.

A fresh WSe$_2$ surface was prepared by exfoliation in air and then immediately transferred to the STM UHV chamber. First, tunnel current-bias voltage (I–V) characteristics were measured using the light-modulated scanning tunneling spectroscopy (STS) method.[21,22] As shown in Fig. 2(a),
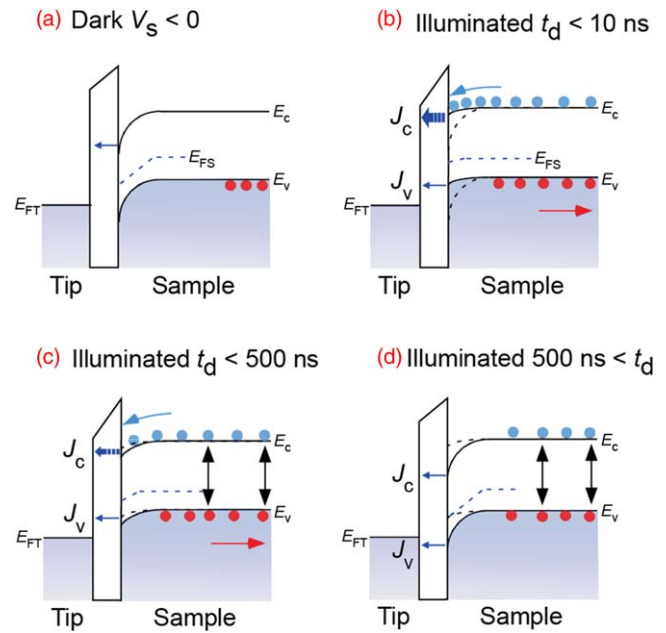
(a)

(b)
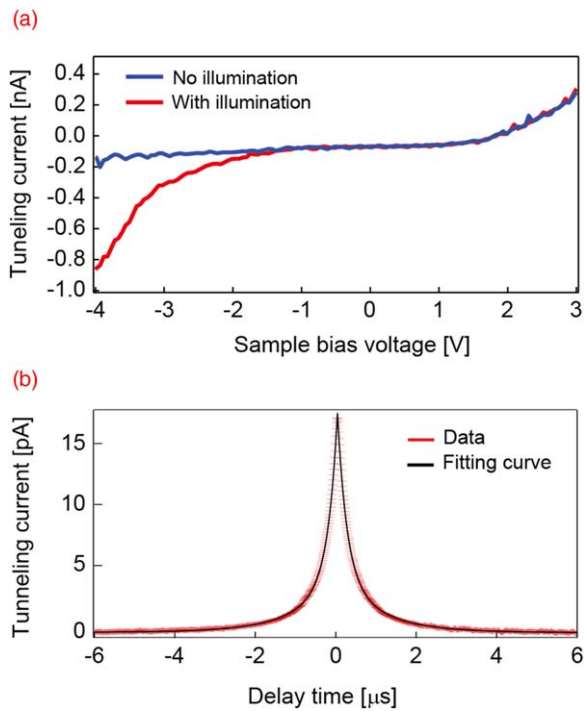
Fig. 2. (Color online) (a) I–V curves obtained by light-modulated STS without (blue) and with (red) laser illumination. Measurements were carried out with a sample bias voltage of $V_s = -3$ V and a setpoint current of $I_{set} = 100$ pA. (b) Typical ET-OPP-STM spectrum obtained for WSe$_2$.

Fig. 3. (Color online) Schematic illustration of band structures of p-type WSe$_2$ samples. (a) Without laser illumination. When the sample is reversely biased ($V_s < 0$), TIBB occurs at the sample surface. (b) Upon laser illumination (here, with a pump pulse), TIBB is reduced owing to charge redistribution, and the tunneling of electrons trapped at the surface occurs. (c) Minority carriers (electrons) that diffuse and drift towards the surface tunnel into the STM tip. Decay process is determined by the balance between the diffusion/drift and tunneling rates. (d) Recombination. E_{FT}, Fermi level of the tip; E_{FS}: Fermi level of the sample; E_v, energy of the valance band edge; E_c, energy of the conduction band edge; J_c: tunneling current contribution from the conduction band; J_v: tunneling current contribution from the valance band.

the I–V curve under laser illumination indicated that the WSe$_2$ sample exhibited typical p-type semiconductor behavior. Namely, the current flow was enhanced by laser illumination under a reverse-bias condition (negative sample bias).

Next, the ET-OPP-STM experiment was carried out. In all measurements, the intensities for the pump and probe lasers were set to be identical and attenuation was realized using natural-density optical filters when necessary. When the laser repetition rate f_{rep} was set to 100 kHz an optical delay time up to 5 μs was provided. The STM bias voltage V_s was set to satisfy the reverse-bias condition ($V_s < 0$). Figure 2(b) shows a typical spectrum obtained by ET-OPP-STM. Two components with lifetimes of 100 ns and μs order were observed. Since the time resolution was ~8 ns, no initial tunneling of extra electrons trapped at the surface was observed, but as expected, we were able to measure the recombination process.

To explain the entire process, a schematic model is shown in Fig. 3. The time-resolved tunneling current measurement is based on the surface photovoltage (SPV) effect.[23] With no laser illumination, downward tip-induced band bending (TIBB)[24,25] occurs in a p-type semiconductor sample under a reversed bias condition ($V_s < 0$), as shown in Fig. 3(a). When the sample is illuminated, namely, a pump pulse arrives at the sample, and the TIBB is reduced owing to the redistribution of the photocarriers. That is, the transient SPV effect consequently increases the effective bias voltage across the tip-sample junction.

After the excitation by the pump pulse, three processes are considered to occur. (1) Initial immediate tunneling of the excess electrons trapped at the surface [Fig. 3(b), ns order]. (2) Minority carrier (electron) diffusion, drift and tunneling on the surface side, where the lifetime is determined by the

balance between the tunneling and diffusion/drift rates [Fig. 3(c), 100 ns order]. (3) Recombination process [Fig. 3(d), μs order].[19] In OPP-STM, the sample surface below the STM tip is excited by a sequence of paired pulses, similar to a conventional OPP method, and the change in tunneling current is measured as a function of the delay time t_d between the pump and probe pulses. The delay time was modulated at 1 kHz for the lock-in detection of a weak signal. The detected signal current is $\Delta I = I(t_d) - I(\infty)$.[26] It is considered that the former two components were observed in the previous OPP-STM, whereas the latter two components were observed in the current ET-OPP-STM measurement.

To further validate this model, we measured the tunneling current dependence of the spectrum. Figure 4(a) shows a series of spectra obtained with different tunneling current setpoints from 10–100 pA. The lifetimes obtained by fitting the data with a double exponential function are presented as a function of setpoint tunneling current in Fig. 4(b) (fast decay component) and 4(c) (slow decay component). It can be seen that when the tip-sample distance was reduced (increasing tunneling current setpoint), the lifetime of the fast component decreased, whereas the lifetime of the slow component was almost constant, which is in good agreement with the proposed model. Namely, a smaller tip-sample distance increases the tunneling rate in the system, which accelerates the fast decay process at the surface, whereas the recombination rate, which determines the decay of the slow component, remains constant regardless of the tunnel current rate.
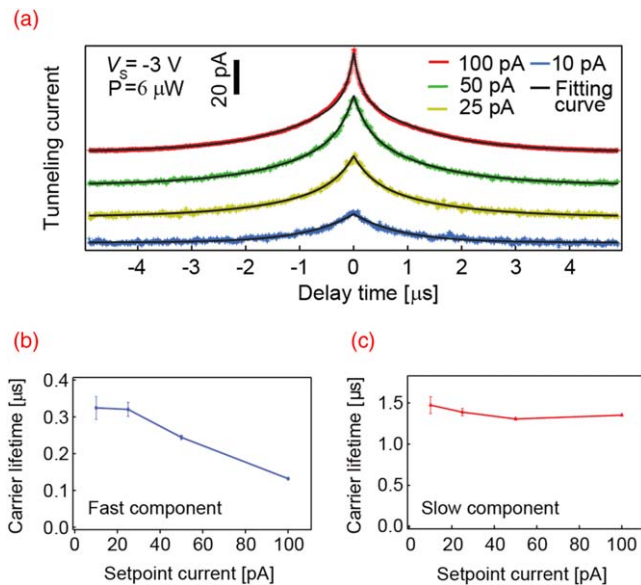
Fig. 4. (Color online) (a) Setpoint tunneling current dependence of the spectrum obtained by ET-OPP-STM ($V_s = -3$ V, 12 μW). Black lines show the fitting curves, where a double exponential function was used. (b) Lifetime of the fast decay component. (c) Lifetime of the slow decay component.

In conclusion, we have developed an applicable type of OPP-STM. Two externally triggerable pulse lasers were used to produce pump and probe pulses, and wide-range delay-time modulation was realized by simply adjusting the timing of electric pulses. The performance of the OPP-STM we have developed was demonstrated by measuring the carrier dynamics in WSe$_2$. In addition to the processes of minority carrier (electron) diffusion and drift, recombination lifetime, which could not be observed by the former OPP-STM measurement, was successfully detected. The easy applicability of the system is expected to lower the barriers to the use of time-resolved STM and play an important role in analyzing local electronic/structural dynamics at nanoscale. For example, in semiconductors such as organic solar cells[27–29] the evaluation of the longer recombination lifetime (μs to ms) is important for band engineering. Also, using externally triggerable lasers with picosecond optical pulse width increases the time resolution of the system, and combined with the polarization modulation technique[30] is highly promising for the realization of spin dynamics measurement by OPP-STM.

1) J. Shah, *Ultrafast Spectroscopy of Semiconductors and Semiconductor Nanostructures* (Springer, Berlin, 1999).
2) A. H. Zewail, Science **328**, 187 (2010).
3) M. K. L. Man et al., Nat. Nanotechnol. **12**, 36 (2017).
4) M. Eichberger, H. Schäfer, M. Krumova, M. Beyer, J. Demsar, H. Berger, G. Moriena, G. Sciaini, and R. J. D. Miller, Nature **468**, 799 (2010).
5) C. J. Chen, *Introduction to Scanning Tunneling Microscopy* (Oxford University Press, Oxford, 2007).
6) H. J. Mamin, H. Birk, P. Wimmer, and D. Rugar, J. Appl. Phys. **75**, 161 (1994).
7) S. Weiss, D. Botkin, D. F. Ogletree, M. Salmeron, and D. S. Chemla, Phys. Stat. Sol. (b) **188**, 343 (1995).
8) J. Wintterlin, J. Trost, S. Renisch, R. Schuster, T. Zambelli, and G. Ertl, Surf. Sci. **394**, 159 (1997).
9) U. Kemiktarak, T. Ndukum, K. C. Schwab, and K. L. Ekinci, Nature **450**, 85 (2007).
10) G. Nunes and M. R. Freeman, Science **262**, 1029 (1993).
11) S. Weiss, D. F. Ogletree, D. Botkin, M. Salmeron, and D. S. Chemla, Appl. Phys. Lett. **63**, 2567 (1993).
12) U. D. Keil, T. Ha, J. R. Jensen, and J. M. Hvam, Appl. Phys. Lett. **72**, 3074 (1998).
13) Y. Terada, S. Yoshida, O. Takeuchi, and H. Shigekawa, J. Phys. Condens. Matter **22**, 264008 (2010).
14) O. Takeuchi, M. Aoyama, R. Oshima, Y. Okada, H. Oigawa, N. Sano, H. Shigekawa, R. Morita, and M. Yamashita, Appl. Phys. Lett. **85**, 3268 (2004).
15) Y. Terada, S. Yoshida, O. Takeuchi, and H. Shigekawa, Nat. Photonics **4**, 869 (2010).
16) P. Kloth and M. Wenderoth, Sci. Adv. **3**, e1601552 (2017).
17) M. Roth, E. Samoka, E. Mojaev, and M. Tseitlin, Proc. Sixth Russian-Israeli bi-National Workshop, p. 205, 2007.
18) M. Yokota, S. Yoshida, Y. Mera, O. Takeuchi, H. Oigawa, and H. Shigekawa, Nanoscale **5**, 9170 (2013).
19) S. Yoshida, Y. Terada, M. Yokota, O. Takeuchi, Y. Mera, and H. Shigekawa, Appl. Phys. Express. **6**, 016601 (2013).
20) C. Sommerhalter, T. W. Matthes, J. Boneberg, P. Leiderer, and M. C. Lux-Steiner, J. Vac. Sci. Technol. B **15**, 1876 (1997).
21) S. Yoshida, Y. Kanitani, R. Oshima, Y. Okada, O. Takeuchi, and H. Shigekawa, Phys. Rev. Lett. **98**, 026802 (2007).
22) S. Yoshida, Y. Kanitani, O. Takeuchi, and H. Shigekawa, Appl. Phys. Lett. **92**, 102105 (2008).
23) R. J. Hamers and D. G. Cahill, J. Vac. Sci. Technol. B **9**, 514 (1991).
24) M. Feenstra, Y. Dong, M. P. Semtsiv, and W. T. Masselink, Nanotechnology **18**, 044015 (2007).
25) S. Yoshida, J. Kikuchi, Y. Kanitani, O. Takeuchi, H. Oigawa, and H. Shigekawa, e-J. Surf. Sci. Nanotech. **4**, 192 (2006).
26) S. Yoshida, Y. Terada, R. Oshima, O. Takeuchi, and H. Shigekawa, Nanoscale. **4**, 757 (2012).
27) C. Vijila et al., J. Appl. Phys. **114**, 184503 (2013).
28) H. Zhou, Q. Chen, G. Li, S. Luo, T. B. Song, H. S. Duan, Z. Hong, J. You, Y. Liu, and Y. Yang, Science **345**, 542 (2014).
29) D. W. De Quilettes, S. M. Vorpahl, S. D. Stranks, H. Nagaoka, G. E. Eperon, M. E. Ziffer, H. J. Snaith, and D. S. Ginger, Science **348**, 683 (2015).
30) S. Yoshida, Y. Aizawa, Z. H. Wang, R. Oshima, Y. Mera, E. Matsuyama, H. Oigawa, O. Takeuchi, and H. Shigekawa, Nat. Nanotechnol. **9**, 588 (2014).